Stimulated Raman scattering in soft glass fluoride fibers

Petersen, Christian; Dupont, Sune; Agger, Christian; Thøgersen, Jan; Bang, Ole; Keiding, Søren Rud

Published in:
Optical Society of America. Journal B: Optical Physics

Publication date:
2011

Document Version
Publisher's PDF, also known as Version of record

Stimulated Raman scattering in soft glass fluoride fibers

Christian Petersen,[1] Sune Dupont,[2] Christian Agger,[3] Jan Thøgersen,[1] Ole Bang,[3] and Søren Rud Keiding[1,*]

[1]*Department of Chemistry, Aarhus University, 8000 Aarhus C, Denmark*
[2]*Department of Physics, Aarhus University, 8000 Aarhus C, Denmark*
[3]*DTU Fotonik, Department of Photonics Engineering, Technical University of Denmark, 2800 Kgs. Lyngby, Denmark*
**Corresponding author: keiding@chem.au.dk*

Received April 5, 2011; revised July 29, 2011; accepted July 30, 2011;
posted August 2, 2011 (Doc. ID 145179); published August 31, 2011

We have measured the absolute Raman gain spectrum in short fluoride soft glass fibers with a pump wavelength of 1650 nm. We found a peak gain of $g_R = 4.0 \pm 2 \times 10^{-14}\,\mathrm{m\,W^{-1}}$.

OCIS codes: 160.2290, 190.5650.

1. INTRODUCTION

Stimulated Raman scattering (SRS) is among the most important of the nonlinear phenomena in optical fibers. The Raman scattering process is, for instance, used for amplification in telecommunication lines and also studied due to its contribution to cross talk between channels [1,2].

Our interest in Raman scattering concerns its involvement in supercontinuum generation in optical fibers [3]. The supercontinuum generation process has been an intense research field over the past few years because of its applicability to octave spanning sources in optical clocks, short pulse generation, and illumination spectroscopy [4–6]. These studies have mainly been performed in silica based fibers, which limits the spectral range to 0.4–2.5 μm. The limited spectral range of silica fibers has led to a growing interest in soft-glass fibers with the aim of generating a mid-infrared supercontinuum [7–9]. The infrared continua being generated by such source are potentially applicable in IR microscopy, free range spectroscopy, and lidars, to mention but a few [10,11]. As simulations are increasingly used to predict the output spectrum of the fiber and to guide the design of new systems, it is paramount that the absolute Raman gain spectrum and its frequency dependence are accurately known. This calls for a precise measurement of the Raman gain spectra of many new materials. A variety of techniques has been used to study the Raman gain. This includes pump–probe techniques [12–15], studying the buildup of the Stokes beam for varying pump pulse length [16], and utilizing the amplification of sidebands through cross-phase modulation (XPM) [17]. Most of these techniques have been used to study either the gain in long fibers or in soft glass fibers with a high value of the Raman gain. Here we present an investigation using pump–broadband probe techniques of the Raman gain spectrum in a step-index fluoride (ZBLAN) fiber.

Mizunami and co-workers previously reported a Raman gain of $g_R = 2.0 \pm 0.5 \times 10^{-13}\,\mathrm{m\,W^{-1}}$ in a ZBLAN fiber. This value was obtained using a nanosecond pump at 580 nm [13]. The shape of the gain spectrum was not shown in that work, but spontaneous scattering spectra have been reported revealing a sharp peak around 600 $\mathrm{cm^{-1}}$ with a plateau extending toward lower values of the Stokes shift [18]. In the present experiment, we use a high-power, ultrashort pump–probe, which makes it possible to determine the Raman gain with short pieces of fiber.

2. EXPERIMENTAL

We determine the Raman gain of ZBLAN by measuring the amplification of a broadband probe in a fiber pumped by a picosecond pulse. The gain is found by recording the probe pulse spectrum after propagation of the fiber with and without the presence of the pump. The on–off probe gain, g_A, is given as

$$g_A(\omega) = \ln\left(\frac{P_{\mathrm{pr}}(\omega)}{P^0_{\mathrm{pr}}(\omega)}\right), \tag{1}$$

where P_{pr} and P^0_{pr} represent the probe power with and without the pump, respectively. The experimental setup is depicted in Fig. 1. The laser system has a central wavelength of 800 nm, a pulse repetition rate of 1 kHz, and 100 fs pulse duration. The 1 mJ output from the amplifier is divided in two equally powerful beams. Each beam pumps an optical parametric amplifier (TOPAS). One of the optical parametric amplifiers (OPAs) generates the pump beam at 1650 nm while the probe is generated in the second OPA. The center wavelength of the probe is 1800 nm. The pump and probe wavelength can be tuned independently. This makes it possible to study the pump wavelength dependence of the Raman gain. The probe has a spectral width of roughly 200 $\mathrm{cm^{-1}}$, and it has a duration of 150 fs. The energy of the probe pulse is negligible compared to the pump. The energy of the pump pulse ranges roughly between 0.5 and 50 nJ, corresponding to peak powers on the order of kilowatts. The pump power can be adjusted using filters and a half-wave plate combined with a broadband polarizer. In order to ensure that the pump and the probe pulses remain temporarily overlapped, the 150 fs pump pulse is stretched by a grating stretcher to $\tau_p = 8$ ps. We will discuss the influence of chirp on the results in Subsection 3.B.

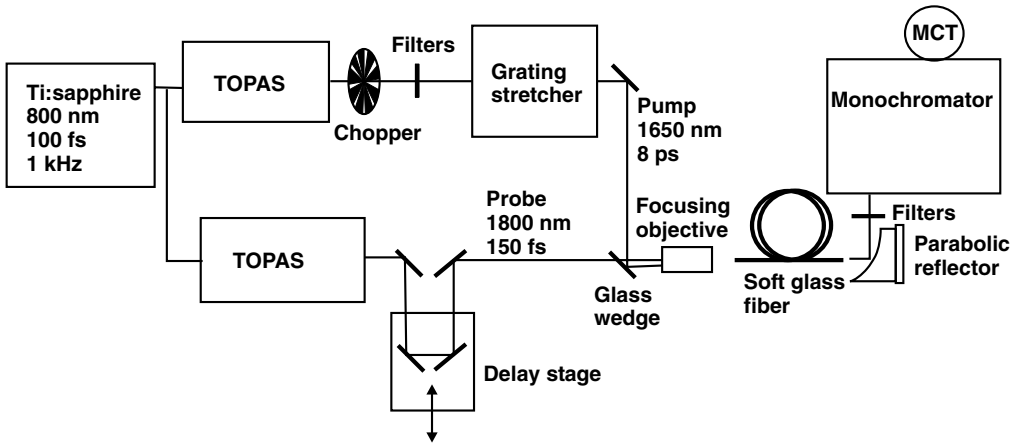

Fig. 1. Schematic drawing of the experimental setup for measuring the gain of the ZBLAN fiber.

The pump passes through a chopper before being coupled into the fiber. The chopper frequency is synchronized to the laser system and blocks every second pump pulse. Consequently, the spectrum of the probe with and without the pump is recorded for consecutive laser pulses.

The pump and probe are overlapped on a glass wedge and copropagate toward the fiber. The pulses are coupled into the fiber using a ×10 microscope objective. After having propagated the length of the fiber, the output is collimated using a gold off-axis parabolic mirror. The off-axis mirror collects both the pump and the probe, and the collimated output is subsequently focused on the entrance slit of a monochromator by a ZnSe lens. The monochromator is equipped with a 32-channel MCT detector.

The soft glass step-index ZBLAN fiber from FiberLabs has a 10.7 μm core with a numerical aperture of 0.2. The zero-dispersion wavelength of the fiber is 1580 nm, and the loss is reported by the manufacturer to be smaller than 60 dB/km for the wavelength range relevant to the present study. The length of the fiber is 35 cm.

The large error in the absolute Raman gain reflects the dependence of the Raman gain on a number of parameters and the difficulty of accurately ascertaining these parameters. For example, in order to know the peak power of the pump inside the fiber, the pulse length, power, effective area, and coupling efficiency have to be established.

3. RESULTS

A. Measured Gain

We have measured the Raman gain in a short piece of ZBLAN fiber using the pump–probe approach described in the previous section. The resulting gain spectrum is shown in Fig. 2 with the gain coefficient on an absolute scale. We find a peak value of $g_R = 4.0 \pm 2 \times 10^{-14}\,\mathrm{m\,W^{-1}}$ at the 1650 nm pump wavelength. The shape of the spectrum is dominated by a narrow peak centered at a Stokes shift of 580 $\mathrm{cm^{-1}}$. A smaller and broader feature extends from the peak toward lower Stokes shifts. The shape closely resembles the shape of the spontaneous scattering spectrum measured by Saïssy *et al.* [18]. The similar shape of the small signal gain spectrum and the spontaneous spectrum is expected from theory [19]. The spectrum can be described as the sum of two Gaussian functions with amplitudes of 0.0352 and 0.0164 nm/kW , center shifts of 580.8 and 414.8 $\mathrm{cm^{-1}}$, and widths of 22.7 and 115.4 $\mathrm{cm^{-1}}$, respectively. This fit is shown with the full line in Fig. 2.

The material gain, g_R, is calculated from the experimentally measured gain, g_A, of the probe. In the continuous wave regime, the material gain relates to the measured amplification of the probe through the following relation:

$$g_R = \frac{g_A}{I_{\mathrm{pu}} L_{\mathrm{eff}}}, \tag{2}$$

where I_{pu} is the peak intensity of the pump and L_{eff} is the effective length of the fiber. To calculate I_{pu} from the peak pump power, we use an effective area, A_{eff}, of 70 $\mu\mathrm{m}^2$ calculated from the core diameter and the dispersion profile. The loss over the length of fiber is less than 1%, and the effective length is thus set equal to the length of the fiber, thereby disregarding loss. Implicit to the use of Eq. (2) is that dispersion and pump depletion are regarded as negligible. To achieve an accurate determination of the gain, we have measured the gain for varying pump power. The gain at the peak Stokes shift as a function of the pump peak power is shown in Fig. 3. The gain shows a clear linear dependence for the recorded peak powers, lending credibility to the assumption of operation in the nondepleted regime of amplification. The shape of the gain spectrum results from linear regression of the power

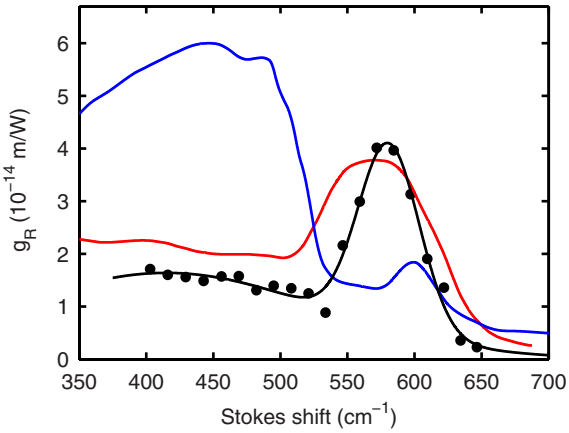

Fig. 2. Raman gain spectrum of the ZBLAN fiber. The points represent the experimental points. The black (lower) curve is a fitted curve consisting of two Gaussian functions (see text for details). The red (middle) curve shows the scaled spontaneous scattering spectrum from the work of Saïssy *et al.* [18]. The blue (upper) curve shows the gain spectrum of silica for comparison [12].

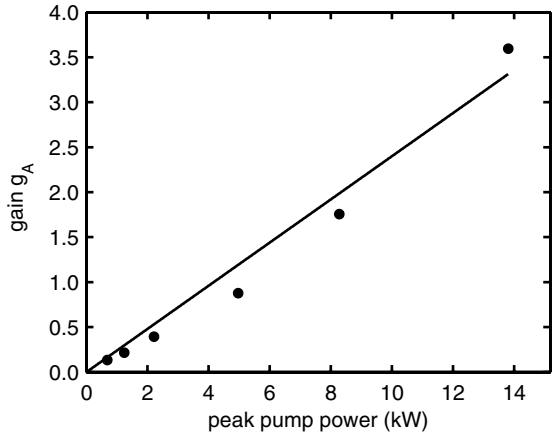

Fig. 3. Stimulated Raman gain as a function of the peak pump power. The points represent the experimentally measured values for a Stokes shift of 580 cm^{-1}. The full line is a linear fit. The slope of the curve corresponds to a material gain of $g_R = 4.0 \times 10^{-14}\,m\,W^{-1}$.

dependence for each separate wavelength with the resulting spectrum shown in Fig. 2.

B. Applicability of the Method

There are several advantages of using pulsed lasers to study the Raman gain in optical fibers. The high powers available in pulsed lasers make it possible to study fiber lengths on the centimeter scale and in fibers with a low Raman gain coefficient. Furthermore, the use of OPAs for pump and probe generation makes the pump wavelength easily tunable. However, using ultrashort pulses in a dispersive fiber has the drawback that the overlap of the pump and probe can vary along the fiber due to walk-off. The walk-off determines the effective interaction length between the pump and probe. The walk-off length can be calculated from the dispersion profile of the fiber as $L_W = T_{pu}/|v_{pu}^{-1} - v_{pr}^{-1}|$, where v_{pu} and v_{pr} are the group velocities of the pump and probe, respectively. For the fiber under consideration here, L_w is found to be roughly 20 m, which is more than 1 order of magnitude longer than the physical length. Consequently, we take the effective length to be equal to the actual length of the fiber. Furthermore, the dispersion length is 4 orders of magnitude longer than the length of the fiber for the pump. For the probe, the dispersion length is calculated to be 75 cm. Thus, the probe will suffer little broadening in the course of the fiber and the pump will be unaffected by dispersion. The respective dispersion lengths have been calculated from the pulse width and the value of β_2 at the central wavelength according to $L_D = T^2/|\beta_2|$, where T is the pulse width. Another concern using ultrashort pulses to quantitatively determine the gain is that the intensity of the pump and probe are so high that nonlinear effects might distort the pulses. To test that this will not cause a flawed result, we have performed simulations under the experimental conditions that confirm that the pump and probe are not significantly distorted along the fiber. The simulations are discussed more in Subsection 3.C. Because of the chirp of the pump, the probe will only overlap with a subset of the frequencies contained in the pump. Changing the delay between pump and probe will therefore move the probe within the pump envelope and effectively change the pump frequency. The measured gain is shown in Fig. 4 as a function of the Stokes shift and as a function of the pump–probe delay on a contour

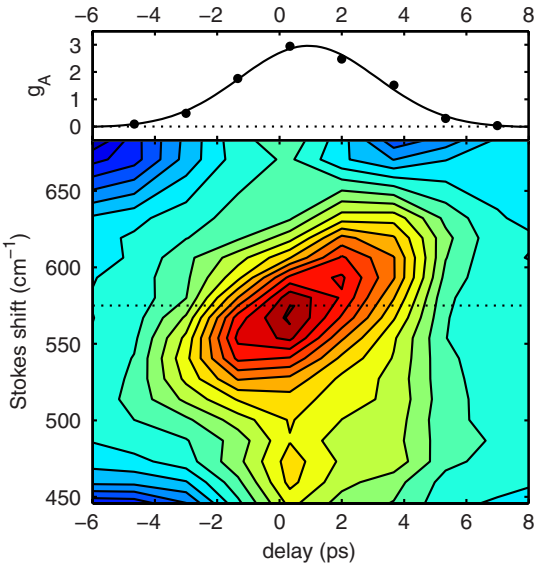

Fig. 4. Raman gain shown as function of the delay between the pump and the probe. The top part of the figure shows the delay dependence at the peak Stokes shift corresponding to a horizontal slice indicated by the dotted line through the contour plot.

plot. The top part of the figure shows a horizontal slice of the plot corresponding to the delay dependence of the Raman gain for a selected Stokes shift. The stimulated Raman gain is present as a diagonal peak in the contour plot. The diagonal profile is caused by the chirp of the pump pulse. The figure shows that the peak of the spectrum moves from smaller to larger Stokes shifts for increasing delays. The negative chirp of the pump means that the frequency decreases from the leading edge to the trailing edge of the pump. For longer delays, the probe is moved toward the leading edge of the pump, meaning that it will interact with a larger effective pump frequency. In the contour plot, an additional signal can be identified at the edge of the gain spectrum. Evidently, this additional signal depends on the overlap between the pump and probe. It is furthermore observed to depend on the intensity of the pump. We interpret this signal as being the realization of XPM between the pump and the probe. The XPM will shift the frequency of the probe. This will give rise to a signal in the pump–probe configuration that is proportional to the derivative of the probe pulse shape and having opposite signs for positive and negative delays, respectively. This feature is also seen to not show signs of the frequency chirp of the pump in correspondence with the fact that XPM is influenced only by the total intensity of the pump modulating the refractive index.

C. Simulations of the Experiment

Because the experimental approach is based on a number of assumptions, we have additionally performed numerical simulations of the pump–probe experiment in order to uncover possible pitfalls in the analysis. In these simulations, pump and probe fields are propagated along the fiber using the generalized nonlinear Schrödinger equation in the interaction picture based on a formalism described in [20]. The Raman response function of the fiber is calculated from the Gaussian fit to the measured gain spectrum, thereby including the full temporal response of the Raman interaction in the simulation. The fraction, f_R, of the nonlinearity related to molecular

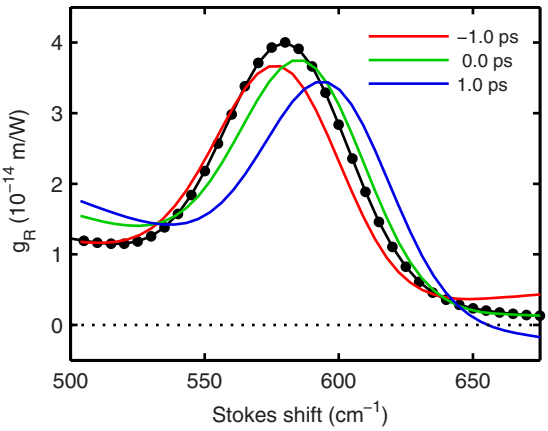

Fig. 5. Raman gain retrieved from the simulations and the Raman gain spectrum input into the simulation (black curve) for zero delay and for a delay of −1 and 1 ps. The pump peak power for this simulation is 500 W.

motion is calculated to be 0.06 based on the Gaussian fit to the spectrum. The parameters of the input fields match the parameters of the optical pulses in the experiment in terms of pulse length and power. The simulations are performed for a pump–probe field and for the probe alone following the procedure of the experiment. The delay between the pump and probe can similarly also be varied in the simulations. From the simulation results, we calculate the spectral density of the output fields similar to what is measured in the experiment. From the spectral density, we then use Eq. (1) to calculate the gain of the probe at the fiber output. Subsequently, the material gain is found using Eq. (2). The difference between this retrieved gain spectrum and the spectrum that initially enters into the simulation is a measure of the validity of the assumptions in the experimental approach. The gain spectra found from analyzing the results of the simulation are shown in Fig. 5 for −1, 0, and 1 ps pump–probe delays. The pump power is 500 W, and the probe peak power 100 W. For all three delays, the calculation of the Stokes shift is based on the central pump wavelength of 1650 nm, thus causing the retrieved spectra for −1 ps and 1 ps delay to be shifted due to the chirp of the pump pulse in correspondence with the experimental observations as shown in Fig. 4. The input gain spectrum based on the experimentally measured gain spectrum is also shown in the figure. The simulations show that for small pump–probe delays, the retrieved spectrum reproduces the input spectrum within the experimental uncertainty, thus supporting the applicability of the continuous wave approach. The deviations from the input spectrum are primarily caused by XPM. As this contribution from XPM depends on the delay between the pump and probe, the retrieved spectrum will also have a time dependence. The best correspondence is found for a small negative delay where the probe is placed slightly before the peak of the pump at the fiber input.

4. CONCLUSION

We have measured the absolute Raman gain of a 35 cm soft glass fluoride fiber using a picosecond pump and determined the shape of the gain spectrum using a broadband probe. The results show a peak gain value of $g_R = 4.0 \pm 2 \times 10^{-14}\,\mathrm{m\,W^{-1}}$ at $580\,\mathrm{cm^{-1}}$ for a pump wavelength of 1650 nm. Finally, the assumption of treating the experiment as a continuous wave experiment thereby neglecting dispersion and nonlinear effects has been investigated and verified with numerical simulations.

ACKNOWLEDGMENTS

We wish to thank the Danish Foundation for Advanced Technology (Højteknologifonden) for financial support.

REFERENCES

1. M. Islam, "Raman amplifiers for telecommunications," IEEE J. Sel. Top. Quantum Electron. **8**, 548–559 (2002).
2. A. R. Chraplyvy, "Optical power limits in multichannel wavelength-division-multiplexed systems due to stimulated Raman scattering," Electron. Lett. **20**, 58–59 (1984).
3. J. M. Dudley, G. Genty, and S. Coen, "Supercontinuum generation in photonic crystal fiber," Rev. Mod. Phys. **78**, 1135–1184 (2006).
4. J. T. Woodward, A. W. Smith, C. A. Jenkins, C. Lin, S. W. Brown, and K. R. Lykke, "Supercontinuum sources for metrology," Metrologia **46**, S277–S282 (2009).
5. C. F. Kaminski, R. S. Watt, A. D. Elder, J. H. Frank, and J. Hult, "Supercontinuum radiation for applications in chemical sensing and microscopy," Appl. Phys. B **92**, 367–378 (2008).
6. B. Schenkel, R. Paschotta, and U. Keller, "Pulse compression with supercontinuum generation in microstructure fibers," J. Opt. Soc. Am. B **22**, 687–693 (2005).
7. P. Domachuk, N. A. Wolchover, M. Cronin-Golomb, A. Wang, A. K. George, C. M. B. Cordeiro, J. C. Knight, and F. G. Omenetto, "Over 4000 nm bandwidth of mid-IR supercontinuum generation in sub-centimeter segments of highly nonlinear tellurite PCFs," Opt. Express **16**, 7161–7168 (2008).
8. G. Qin, X. Yan, C. Kito, M. Liao, C. Chaudhari, T. Suzu, and Y. Ohishi, "Supercontinuum generation spanning over three octaves from UV to 3.85 μm in a fluoride fiber," Opt. Lett. **34**, 2015–2017 (2009).
9. J. Hu, C. R. Menuyk, L. B. Shaw, J. S. Sanghera, and I. D. Aggarwal, "Maximizing the bandwidth of supercontinuum generation in As_2Se_3 chalcogenide fibers," Opt. Express **18**, 6722–6739 (2010).
10. P. Garidel and M. Boese, "Mid infrared microspectroscopic mapping and imaging: a bio-analytical tool for spatially and chemically resolved tissue characterization and evaluation of drug permeation within tissues," Microsc. Res. Tech. **70**, 336–349 (2007).
11. G. Mejean, J. Kasparian, E. Salmon, J. Yu, J.-P. Wolf, R. Bourayou, R. Sauerbrey, M. Rodriguez, L. Wöste, H. Lehmann, B. Stecklum, U. Laux, J. Eislöffel, A. Scholz, and A. P. Hatzes, "Towards a supercontinuum-based infrared lidar," Appl. Phys. B **77**, 357–359 (2003).
12. R. H. Stolen and E. P. Ippen, "Raman gain in glass optical waveguides," Appl. Phys. Lett. **22**, 276–278 (1973).
13. T. Mizunami, H. Iwashita, and K. Takagi, "Gain saturation characteristics of Raman amplification in silica and fluoride glass optical fibers," Opt. Commun. **97**, 74–78 (1993).
14. D. J. Dougherty, F. X. Kärtner, H. A. Haus, and E. P. Ippen, "Measurement of the Raman gain spectrum of optical fibers," Opt. Lett. **20**, 31–33 (1995).
15. R. E. Slusher, G. Lenz, J. Hodelin, J. Sanghera, L. B. Shaw, and I. D. Aggarwal, "Large Raman gain and nonlinear phase shifts in high-purity As_2Se_3 chalcogenide fibers," J. Opt. Soc. Am. B **21**, 1146–1155 (2004).
16. D. Mahgerefteh, D. L. Butler, J. Goldhar, B. Rosenberg, and G. L. Burdge, "Technique for measurement of the Raman gain coefficient in optical fibers," Opt. Lett. **21**, 2026–2028 (1996).
17. A. Tuniz, G. Brawley, D. J. Moss, and B. J. Eggleton, "Two-photon absorption effects on Raman gain in single mode As_2Se_3 chalcogenide glass fiber," Opt. Express **16**, 18524–18534 (2008).
18. A. Saïssy, J. Botineau, and L. Macon, "Diffusion Raman dans une fibre optique en verre fluoré," J. Phys. Lett. **46**, 289–294 (1985).
19. A. Yariv, *Quantum Electronics* (Wiley, 1975).
20. J. Laegsgaard, "Mode profile dispersion in the generalized nonlinear Schrödinger equation," Opt. Express **15**, 16110–16123 (2007).